

# A Three-Transistor Threshold Voltage Model for Halo Processes

Rafael Rios, Wei-Kai Shih, Atul Shah, Sivakumar Mudanai,  
Paul Packan, Tracy Sandford, and Kaizad Mistry

Portland Technology Development, Intel Corporation, Hillsboro, OR 97124, USA

## Abstract

A closed-form expression for the threshold voltage,  $V_t$ , of MOSFETs fabricated with halo processes is described. The proposed approach accurately captures the length dependent  $V_t$  behavior under different drain and body bias conditions and temperature. In addition, the necessity of considering separate  $V_t$  expressions for current and capacitances is discussed. A doping transformation is employed to obtain equivalent channel dopings, necessary for charge-sheet models that do not rely on the threshold voltage concept.

## 1. Introduction

Current MOSFET technologies make use of halo or pocket implants [1-3] for improved scaling and control of short-channel effects. These processes result in non-uniform channel doping profiles along the device length, as illustrated in Fig. 1, which in turn gives rise to the well known reverse short-channel effect (RSCE). A closed-form  $V_t$  solution for non-uniform lateral doping profiles is not trivial. The few models that have appeared in the literature [4-6] are empirical and do not capture the physical RSCE behavior observed in strong halo processes. In addition, the different behaviors of I-V and C-V characteristics for halo processes have not yet been discussed in the literature.

The lack of a good RSCE model as a function of channel length is one of the leading causes for the need for multiple model parameter sets for circuit simulations, using the so-called parameter binning approach [6]. Parameter binning suffers from many drawbacks, including the time and effort to generate model parameters, lack of scalability, problems with smoothness, etc. This is illustrated in Fig. 2 by fitting  $V_t$  using BSIM4's binning approach.

Here, we propose a more physical RSCE model that enables accurate fits to the channel length dependency without the need for parameter binning.

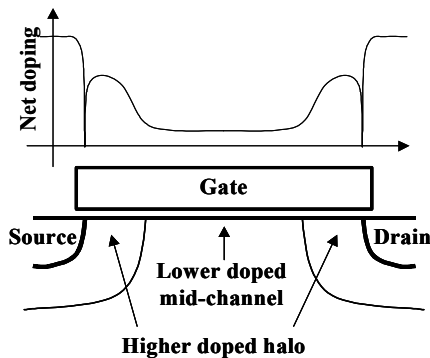


Fig. 1: Illustration of non-uniform channel doping resulting from typical halo processes.

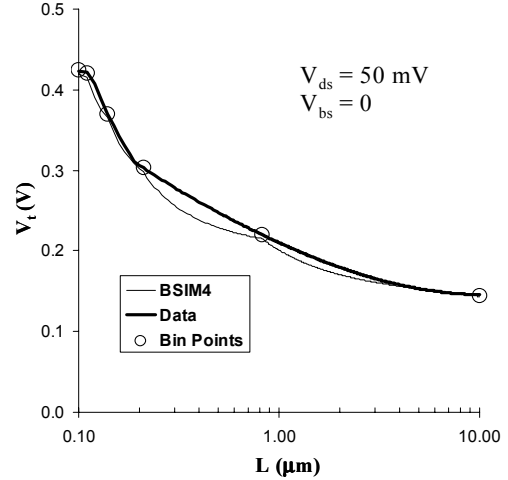


Fig. 2:  $V_t$  fits using the binning approach of BSIM4. The accuracy and smoothness of the fits are strongly dependent on the number and location of bin points.

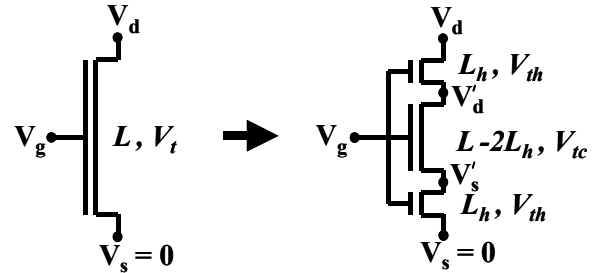


Fig. 3: Schematic representation of the device as formed by a center device with threshold  $V_{ic}$ , bounded by two edge devices of length  $L_h$  and threshold  $V_{th}$ .

## 2. Model description

The effect of the non-uniform lateral doping can be approximated by considering a composite device formed by three transistors in series, as illustrated in Fig. 3, with a center device with low threshold,  $V_{ic}$ , bounded by two edge devices with higher threshold,  $V_{th}$ . The series connection of the three transistors is considered for the channel current. To find the threshold voltage of the composite device for I-V, the sub-threshold currents are matched, resulting in a system of three independent equations with the unknowns  $V_t$ ,  $V'_d$  and  $V'_s$ :

$$\begin{aligned} \frac{e^{-\beta V_t}}{L} (1 - e^{-\beta V_d}) &= \frac{e^{-\beta V_{th}}}{L_h} (1 - e^{-\beta V'_s}) \\ &= \frac{e^{-\beta V_{ic}}}{L - 2L_h} (1 - e^{-\beta (V'_d - V'_s)}) = \frac{e^{-\beta V_{ic}}}{L_h} (1 - e^{-\beta (V_d - V'_d)}) \end{aligned} \quad (1)$$

where  $\beta$  is the inverse of the thermal voltage  $v_T = kT/q$ .

Solving (1) for  $V_t$  leads to the following expression, valid for  $L > 2L_h$ :

$$V_{t(I-V)} = V_{tc} + v_T \ln \left[ 1 + \frac{2L_h}{L} \left( e^{\beta(V_{th}-V_{tc})} - 1 \right) \right] \quad (2)$$

For the device quasi-static capacitance, we must consider the parallel connection of the devices in Fig. 3. Equating the sum of the sub-threshold inversion charges leads to:

$$V_{t(C-V)} = V_{tc} - v_T \ln \left[ 1 + \frac{2L_h}{L} \left( e^{-\beta(V_{th}-V_{tc})} - 1 \right) \right] \quad (3)$$

For charge-sheet, surface potential based models, that do not use threshold voltage explicitly, we can find equivalent dopings for the composite device using the doping transformation:

$$N_a = \frac{(\epsilon_{ox} V_t)^2}{4q\epsilon_{si} t_{ox}^2 \phi_f} \quad (4)$$

obtained directly from the depletion charge contribution. Using (4), and ignoring the weak doping dependency of the band-bending  $\phi_f$ , the equivalent dopings for any given channel length are given by:

$$N_a = \begin{cases} \sqrt{N_c + \frac{sv_T}{\delta} \ln \left[ 1 + \frac{2L_h}{L} \left( e^{s\delta(\sqrt{N_h/2+N_c} - \sqrt{N_c})/v_T} - 1 \right) \right]}^2, & L \geq 2L_h \\ N_c + N_h \frac{L_h}{L}, & L_h < L < 2L_h \\ N_c + N_h \left( 2 - \frac{L}{L_h} \right), & L \leq L_h \end{cases} \quad (5)$$

$$\delta = 2 \frac{t_{ox} \sqrt{q\epsilon_{si} \phi_f}}{\epsilon_{ox}}$$

$$s = \begin{cases} 1 & \text{for I-V} \\ -1 & \text{for C-V} \end{cases}$$

where  $N_c$  and  $N_h$  are the average dopings of the center and halo regions, respectively. To arrive at the expressions valid for  $L < 2L_h$ , the additional assumption that the halo doping varies linearly within the length  $L_h$  has been used.

Within the assumptions of the three-transistor approximation, the model maintains the correct dependencies for the three physical parameters: background doping  $N_c$ , halo doping  $N_h$ , and halo characteristic length  $L_h$ . Most importantly, the model includes physical dependencies to gate oxide thickness,  $t_{ox}$ , and temperature,  $T$ , which are essential to preserve the model scalability.

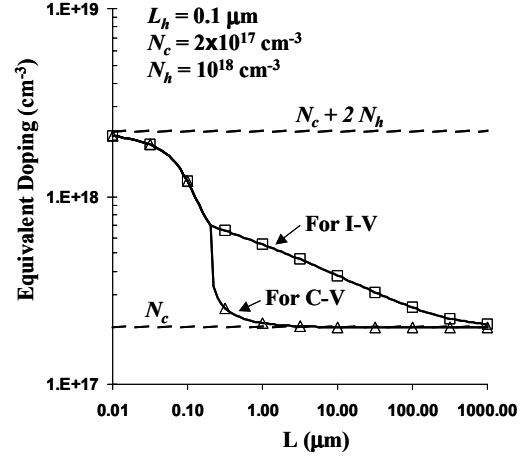


Fig. 4: Example of equivalent channel dopings for I-V and C-V, as given by the expressions (5).

### 3. Results

Fig. 4 illustrates the length dependency of the equivalent channel dopings for I-V and C-V. For channel lengths  $> 2L_h$  (when the low-doped center region becomes exposed) the threshold voltage and corresponding equivalent doping for C-V drops very quickly, accounting for the quasi-static buildup of inversion charge in the center device before there is significant lateral conduction.

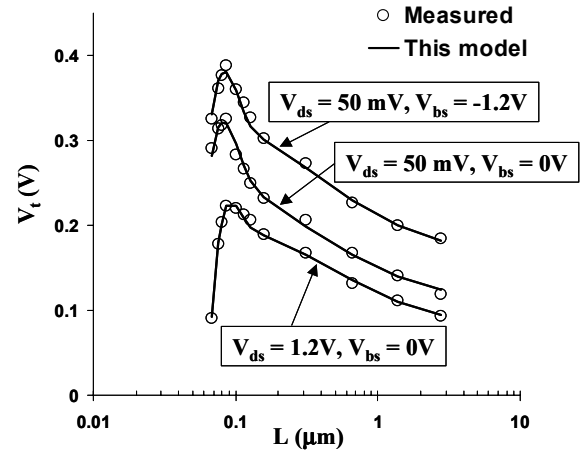


Fig. 5: Model fit to  $V_t$  data with a relatively large RSCE effect. The proposed approach captures the correct length dependencies for all bias conditions.

The proposed RSCE model was combined with a short-channel effect (SCE) model similar to the one described in [7] and implemented in Intel's in-house compact MOSFET model. The accuracy of the model is illustrated in Fig. 5 by fitting  $V_t$  data for the 130 nm technology node [8]. The proposed model shows excellent fits despite of the relatively large RSCE of these devices. As a benchmark, the industry standard model BSIM4 was also fitted to the same data using a single parameter set (no binning), as shown in Fig. 6. The empirical RSCE model of BSIM4 results in a parabolic shape

in the  $\log(L)$  plot and cannot capture the distinct behavior seen in the measured data. Note that this parabolic behavior is also observed between the bin points of Fig. 2, due to the  $1/L$  dependencies of the binning equations.

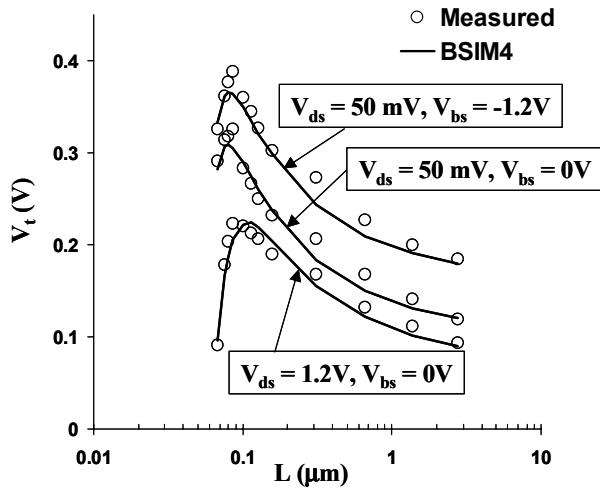


Fig. 6: BSIM4 fits to the same data of Fig. 5. The BSIM4 model does not capture the correct length dependent shape.

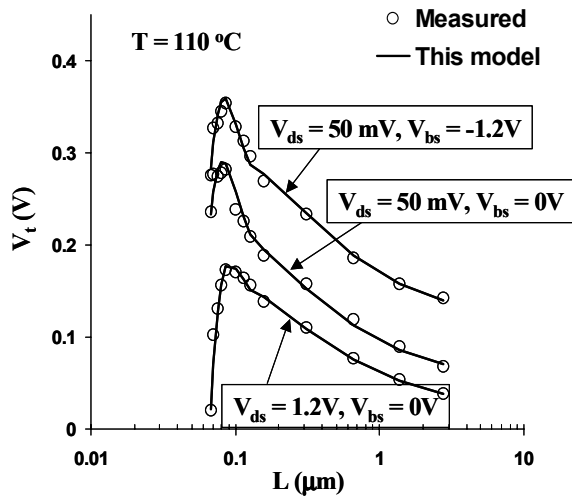


Fig. 7: High temperature fit for the same devices of Fig. 5 with no additional temperature parameters for RSCE.

Fig. 7 illustrates the model's physical nature by fitting the high temperature  $V_t$  data for the same devices of Fig. 5 with no additional temperature parameters.

The need for different  $V_t$  models for I-V and C-V for intermediate size devices is illustrated in Fig. 8. The center device begins to form an inversion layer near  $V_{gs} = 0$ , indicated by the increase in gate capacitance, before there is significant current conduction along the channel. Using the same  $V_t$  model for I-V and C-V results in large errors in the C-V characteristics, as depicted by the solid lines in Fig. 8. Using the separate equivalent doping model for C-V given in

expressions (5) results in excellent fits for the quasi-static C-V, as shown by the dashed lines in the figure.

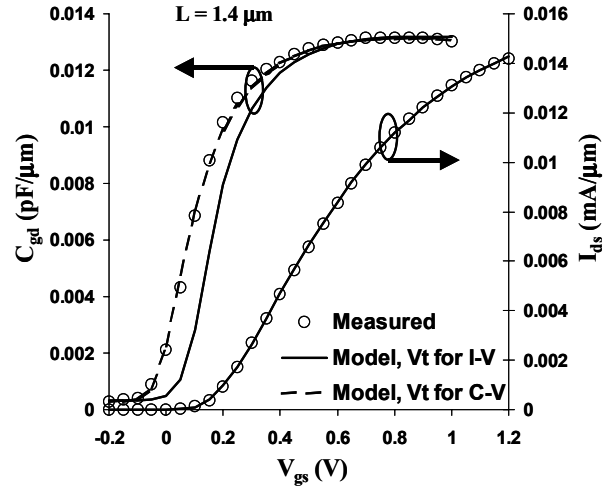


Fig. 8: Fits to linear region current  $I_{ds}$  and quasi-static split capacitance  $C_{gd}$  for an intermediate size device, illustrating the need for a separate  $V_t$  model for C-V.

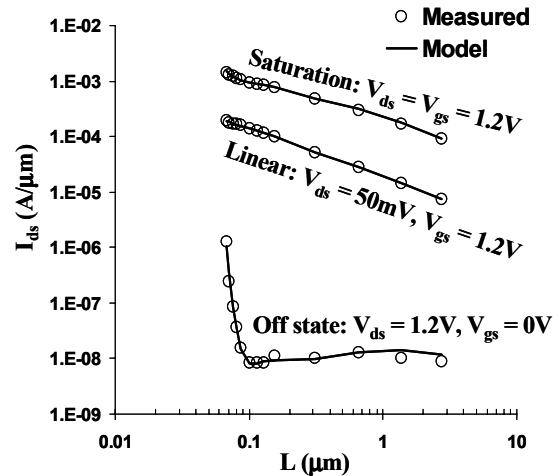


Fig. 9: Compact model fits to linear, saturation, and off-state leakage currents using a single parameter set.

When applied to a physical compact MOSFET model, the proposed approach enables excellent fits for all channel lengths with a single model parameter set. This is illustrated in Fig. 9 by the good fits to the saturation, linear, and off-state leakage currents for a wide range of channel lengths.

#### 4. Beyond the Single $V_t$ Model

The RSCE model discussed in section 2 describes an equivalent  $V_t$  (or equivalent channel doping) for halo devices that can be used in standard single  $V_t$  (or charge-sheet) compact models. However, just finding an equivalent  $V_t$  may not be sufficient to accurately describe the device behavior. Strong halo devices also have peculiar characteristics that

present challenges for modeling and characterization. Some of these are discussed below.

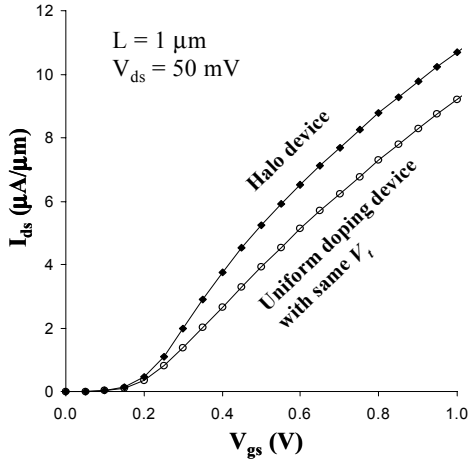


Fig. 10: Simulated linear region characteristics of two devices of same  $V_t$  with halo doping (dark symbols) and uniform channel doping (white symbols).

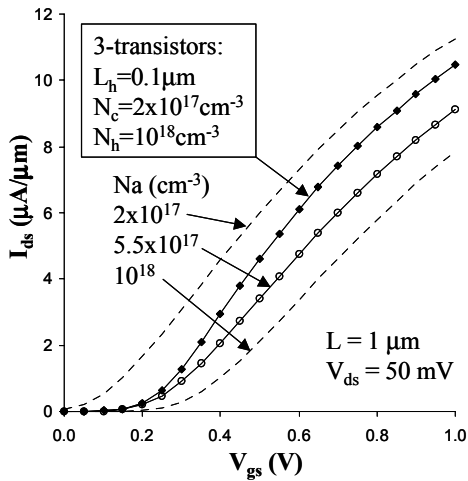


Fig. 11: 3-transistor equivalent used to reproduce and understand the halo effect on the linear current behavior.

### A. Device Characteristics

Fig. 10 shows linear region characteristics of two devices with same length and matched  $V_t$ , obtained with 2-D device simulations. One device has a non-uniform halo profile while the other has a uniform channel doping. The halo device shows increased peak trans-conductance and higher strong inversion currents. This behavior difference is easily understood by using the 3-transistor equivalent model depicted in Fig. 3. The behavior of the equivalent 3-transistor model, obtained with a circuit simulator, is compared to that of a single device with same  $V_t$ , in Fig. 11. The dashed lines represent the two extremes of devices with uniform  $N_c$  and  $N_h$  dopings, which help clarify the halo effect on the device behavior. The heavily doped halo region impacts the weak inversion, since the device turn-on characteristics is limited

by the available carriers in the higher  $V_t$  halo region. Once strong inversion sets in, the low doping, low  $V_t$ , center region begins to dominate resulting in larger currents than that of a uniformly doped device. The higher currents are simply due to increased gate drive, or reduced channel resistance, in the center region.

This analysis suggests that applying the standard single  $V_t$  models to analyze devices with strong halo dopings may lead to incorrect results. A more appropriate analytic model can be derived from the series resistance connection of the three channel regions, assuming strong-inversion condition and constant mobility:

$$I_{ds} = \frac{\mu \cdot C_{ox} \cdot W \cdot V_{ds}}{\frac{2 \cdot L_h}{V_{gs} - V_{th} - 0.5 \cdot V_{ds}} + \frac{L - 2 \cdot L_h}{V_{gs} - V_{tc} - 0.5 \cdot V_{ds}}}$$

This simple model shows how the higher gate drive  $V_{gs} - V_{tc}$  of the center region should result in higher currents. Unfortunately, use of the above expression requires characterization of the parameters  $L_h$ ,  $V_{th}$ , and  $V_{tc}$ .

### B. Apparent Mobility Enhancement/Degradation

Another implication of Figs. 10 and 11 is that data analysis with standard single  $V_t$  models will lead to overestimated long-channel mobility values. On the other hand, the overestimated long-channel mobility will lead to apparent mobility degradation for short-channel devices. Furthermore, mobility extractions based on split C-V techniques become compromised by the different  $V_t$  of I-V and C-V (see Fig. 8).

### C. Non Quasi-static (NQS) Behavior

Fig. 8 shows the quasi-static or low frequency C-V behavior, where enough time is given for the buildup of inversion charge. At high frequencies or fast gate voltage ramps, the higher  $V_t$  of the halo region will have the effect of further damping the formation of the inversion layer.

## Conclusion

The simple three-transistor approximation results in a physical compact model for RSCE, enabling accurate  $V_t$  fits to all channel lengths with a single model parameter set. Distinct  $V_t$  expressions for I-V and C-V are proposed, essential for correct modeling of devices longer than twice the halo characteristic length. In addition, potential implications for the modeling and characterization of devices fabricated with strong halo processes have been discussed.

## References

- [1] Y. Okumura, et al., IEDM Tech. Dig., p.391, 1990.
- [2] T. Hori, IEDM Tech. Dig., p.75, 1994.
- [3] Y. Taur, et al., IEDM Tech. Dig., p. 215, 1997.
- [4] X. Zhou, et al., TED-47, p.214, Jan 2000.
- [5] M. Miura-Mattausch, et al., TED-48, p.2449, Oct 2001.
- [6] BSIM4 User's Manual, www-device.eecs.berkeley.edu
- [7] B. Iniguez, TED-42, p. 1712, Sept 1995.
- [8] S. Tyagi, et al., IEDM Tech. Dig., p. 567, 2000